THE JOURNAL OF PHYSICAL CHEMISTRY B

Article

pubs.acs.org/JPCB

W/O Microemulsions as Dendrimer Nanocarriers: An EPR Study

Shifra Rokach,[†,⊥] Maria Francesca Ottaviani,*[,‡] Alexander I. Shames,[§] Ido Nir,[¶] Abraham Aserin,[†] and Nissim Garti*[,†]

[†]The Ratner Chair of Chemistry, Casali Institute of Applied Chemistry, The Institute of Chemistry, The Hebrew University of Jerusalem, Edmond J. Safra Campus, Givat Ram, Jerusalem 91904, Israel

[‡]Department of Earth, Life and Environment Sciences, University of Urbino, Loc. Crocicchia, Urbino 61029, Italy

[§]Department of Physics, Ben-Gurion University of the Negev, P.O. Box 653, Beer-Sheva 84105, Israel

[¶]The Israel Institute for Biological Research, P.O. Box 19, Ness-Ziona 74100, Israel

ABSTRACT: A complex system, based on a dendrimer solubilized in the aqueous core of water-in-oil microemulsion, may combine the advantages of both dendrimers and microemulsions to provide better control of drug release. We report for the first time the use of EPR technique to determine the effect of solubilized dendrimer on the structure of the microemulsion. The solubilized poly(propyleneimine) (PPI-G2) interacts with sodium bis(2-ethylhexyl) sulfosuccinate (AOT). EPR analysis provided information on polarity, microviscosity, and molecular order of the systems. Polarity and microviscosity increased from unloaded water-in-oil microemulsion to the system loaded with 0.2 wt % PPI-G2, but remained unchanged with higher PPI-G2 loads. The degree of order also increased with 0.2 wt % PPI-G2 with only minor additional increase with larger quantities (25 wt %) of PPI-G2. Variations in pH only slightly affected the structure of microemulsion in the absence and presence of the loaded dendrimers. Aliphatic oils with longer lipophilic chains enhanced the structural order of the microemulsion. On increasing water content, polarity and degree of order increased. PPI-G2 dendrimer in small loads is attracted by the negatively charged AOT and thus intercalates in the interface of the droplets. Yet, at higher PPI-G2 loads, the excess molecules are solubilized in the water core.

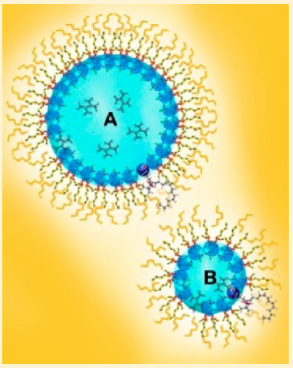

1. INTRODUCTION

Water-in-oil (W/O) microemulsions (MEs) are thermodynamically stable, macroscopically homogeneous, and optically transparent systems of water nanodroplets dispersed into apolar solvents in the presence of adequate surfactants.[1−4] MEs are formed by reducing the oil/water interfacial tension to ultralow values by means of a surfactant or, more commonly, a mixture of surfactants and cosurfactants, thereby allowing thermal motions to spontaneously disperse the two immiscible phases. The typical size of ME droplets is in the range of 5−100 nm.[5,6]

MEs have been extensively studied as drug delivery nanocarriers due to their special features: nanometric size, low viscosity, thermal and thermodynamic stability, ease of preparation, high solubilization capacity, and good bioavailability.[2,6−9]

Due to its double-tailed nature, sodium bis(2-ethylhexyl) sulfosuccinate (AOT) is one of the few ionic surfactants that forms MEs without addition of any cosurfactants.[2] In addition, AOT systems allow control over the size of the spherical water core. For a given surfactant concentration the droplet radius increases linearly with increasing water content.[9]

Since the beginning of the 1990s there has been a widely increasing interest in the biological, (bio)medical, and pharmaceutical applications of dendrimers.[8−12] Dendrimers are globular macromolecules that have a treelike hyperbranched structure, a well-defined molecular weight, and a large number of peripheral groups.[11] However, the first and second generation dendrimers are small and have an open and extended structure.[13]

Dendrimers have narrow polydispersity and nanometer size range, which can allow easier passage across biological barriers. These properties make dendrimers suitable as host−guests for drugs.[12,14] Host−guests are either entrapped in the interior of the dendrimer architecture (electrostatic, hydrophobic, and hydrogen bond interactions) or conjugated to the peripheral groups (electrostatic interactions and covalent bonding).[11,15,16] The presence of multiple terminal groups on the exterior of the dendrimer offers an excellent platform for the attachment of drugs, cell-specific targeting groups, solubility modifiers and stealth moieties,[11] and genes.[17,18]

Dendrimers themselves can serve as therapeutic agents by virtue of their activities[19] against prion diseases,[20] Alzheimer disease,[21] inflammations,[22] human immunodeficiency virus (HIV),[23] herpes simplex virus (HSV),[24] bacteria,[25] cancer, and others.[26] Dendrimers prevent formation of amyloid fibrils and disaggregate previously formed fibrils,[21,27,28] thus preventing viral adhesion and replication.[23]

Poly(propyleneimine) polycationic dendrimers are of particular interest since they are biocompatible and commercially available.[12,29,30] Polycationic dendrimers were shown to react with bacterial membranes and disturb their integrity.[31] The

Received: August 1, 2012
Published: September 18, 2012

   dx.doi.org/10.1021/jp307616b | J. Phys. Chem. B 2012, 116, 12633−12640

second generation poly(propyleneimine) dendrimer (PPI-G2; Chart 1A) possesses eight primary amine groups on the surface

Chart 1. Chemical Structures of (A) Second Generation Poly(propyleneimine) (PPI-G2) and (B) 5-Doxylstearic Acid (5-DSA)

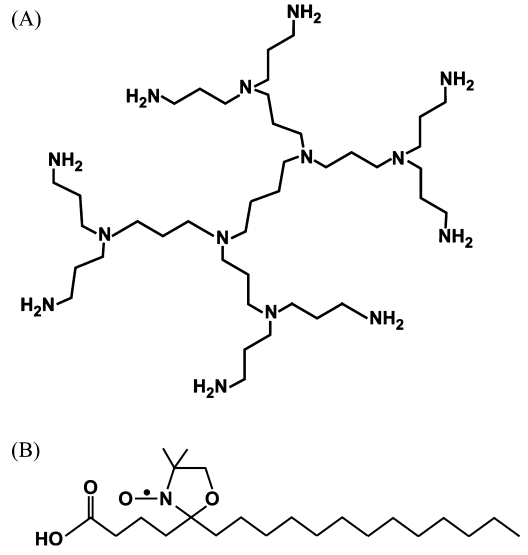

and has a spherical shape with a radius of gyration between 6−7 Å.[32,33] In aqueous solution at pH < 9.85, most of the PPI-G2 terminal amine groups are protonated and have positive surface charges.[33]

Nir et al.[33] proposed a complex drug delivery system based on a dendrimer solubilized in the aqueous core of a W/O ME. This approach may combine the advantages of both dendrimers and MEs, to provide better control of drug release. In this research, PPI-G2 dendrimer was solubilized into the water core of a W/O ME composed of AOT, heptane, and water. It was demonstrated that at constant aqueous phase content (24 wt %) up to 25 wt % of PPI-G2 (from the aqueous phase) could be solubilized into the ionic AOT-based ME (130/1 water/PPI-G2 molar ratio). When (5−25 wt %) dendrimer is solubilized in the water core, the diameter of the droplets is 8.5−9.8 nm. Considerable water binding by PPI-G2, accompanied by partial dehydration of AOT polar heads, was detected by ATR-FTIR and DSC analysis, suggesting that PPI-G2 acted as a "water pump" that caused competition for interfacial water binding between PPI-G2 and AOT.[33]

Electron paramagnetic resonance (EPR) technique is a powerful spectroscopic tool examining some important structural and dynamic parameters affected by the MEs loaded with PPI-G2, which provides information on polarity $\langle A \rangle$, microviscosity (τ_{perp}), and molecular order (S) of the W/O MEs[34,35] as a function of structural compositional parameters such as pH, type of oil, and water content.

In this study, we selected 5-doxylstearic acid (5-DSA; Chart 1B) as a probe that is embedded into the surfactant layer[10,36−39] and therefore reports about interactions between PPI-G2, water, and AOT. Such knowledge helps to visualize where and how the dendrimer is solubilized in the W/O ME droplets and whether it influences the structure of these systems.

2. MATERIALS AND METHODS

2.1. Materials. Sodium bis(2-ethylhexyl) sulfosuccinate (99% purity), *n*-heptane (>99% purity), *n*-decane (>99% purity), dodecane (>99% purity), and 5-doxylstearic acid [2-(3-carboxypropyl)-4,4-dimethyl-2-tridecyl-3-oxazolidinyloxy] (Chart 1B), free radical, were purchased from Sigma-Aldrich (St. Louis, MO). PPI-G2 (>95% purity; Chart 1A), was obtained from SyMO-Chem, The Netherlands. Hydrochloric acid (37%) was purchased from Bio-Lab Ltd. (Jerusalem, Israel). Water was double distilled. All ingredients were used without further purification.

2.2. Preparation of the Microemulsions. The AOT-based MEs were prepared by adding the aqueous phase (solution with or without PPI-G2 in water) to a binary mixture of AOT and oil (1:1.5 weight ratio). Each sample was mixed by vortexing. The aqueous phase content in the ME samples was 13 wt % or 24 wt % at different pH values, and three different oil phases (heptane, decane, and dodecane), while the PPI-G2 content in the aqueous phase was 0−25 wt %.

2.3. Electron Paramagnetic Resonance (EPR) Measurements. *2.3.1. Insertion of the Probe.* The 5-DSA probe was first dissolved in chloroform at a concentration of 2.5×10^{-3} M. An appropriate quantity of the probe solution was placed in tubes, and the solvent was then evaporated before the MEs were prepared within these tubes. A low concentration of 4×10^{-5} M probe in the examined ME systems has already been demonstrated to not perturb similar nanostructures.[34,35,40]

2.3.2. EPR Instrumentation and Method. Room temperature (T = 295 ± 1 K) EPR measurements were carried out using a Bruker EMX-220 X-band ($\nu \sim 9.4$ GHz) equipped with Oxford ESR 900 temperature accessories and an Agilent 53150A frequency counter. The EPR experiment setup includes a nonsaturating MW power of 20 mW, modulation amplitude of 1 G, MW frequency of 9.465 GHz, center magnetic field of 3369.85 G, sweep width of 200.00 G, resolution of 1024 points, time constant of 1.28 ms, and conversion time of 20.48 ms, with a coherent acquisition of 49 scans per each EPR spectrum.

2.3.3. Computation of the EPR Spectra. The computer-aided analysis of the EPR spectral line shape was performed by means of the well-established procedure of Budil et al.[41] and Schneider and Freed.[42] The EPR spectra of 5-DSA in solution was constituted by the three hyperfine lines (due to the coupling between the unpaired electron spin, S = 1/2, and the nitrogen ^{14}N nuclear spin, I = 1) at almost the same intensities. The main parameters that monitor the structural and dynamic modifications of the 5-DSA environment in the different experimental conditions are the following. (a) The perpendicular component of the correlation time for the rotational motion (τ_{perp}). This parameter increased with the decrease in 5-DSA mobility, that is, with the increase in the microviscosity of the probe environment. The jump or the Brownian rotational diffusion models were used, for which $\tau_{perp} = 1/D$ and $1/6D$, respectively, where D is the rotational diffusion coefficient. (b) The average hyperfine coupling constant, $\langle A \rangle = (A_{xx} + A_{yy} + A_{zz})/3$, for the coupling between the electron spin and the nuclear spin, changed as well from system to system, monitoring the variation in the environmental polarity of the probe and, eventually, the anisotropy of the coupling. (c) When the probe is inserted in an ordered lipid layer, the molecular order parameter (S) extracted from computation monitors the order degree, being S = 0 for a completely disordered system and S = 1 for an ordered one.

3. RESULTS AND DISCUSSION

Kabanov et al.[43] estimated the primary PPI-G2 amine groups' pK^p and tertiary amine groups' pK^t to be 9.85 and 6, respectively. This means that at pH 13 the terminal groups of PPI-G2 are unprotonated and, when PPI-G2 is titrated with HCl to pH 8.6 most of the terminal groups are protonated (NH_3^+), thus enhancing the interactions between the positively charged PPI-G2 terminal groups and the negatively charged AOT headgroups. The EPR spectra of 5-DSA have already shown to report about the structural variations of surfactant aggregates due to interactions with dendrimers in different protonating conditions.[38] It seems therefore that the EPR technique is an adequate method to investigate the effect of PPI-G2 solubilization on the ME.

PPI-G2 was solubilized into the ternary AOT/heptane/water system at two different compositions. The first system was relatively rich in water content (constant 24 wt % aqueous phase) at pH 13, with dendrimer concentration from 5 to 25 wt % of the aqueous phase. At PPI-G2 concentrations >25 wt % the MEs separated, after a short storage period, into two isotropic phases. The second system was poor in water (constant 13 wt %) with 5 wt % PPI-G2 (from aqueous phase), at two pHs (13 and 8.6). It should be noted that at low pH (pH 8.6) the maximum load of water was 13 wt %, which resulted in solubilization of 5 wt % PPI-G2. Above this concentration of water or PPI-G2, the MEs are not stable. This is due to strong interactions between the negatively charged AOT headgroups and the positively charged PPI-G2 terminal amine groups at pH 8.6.

Polarity $\langle A \rangle$, microviscosity (τ_{perp}), and molecular order parameter (S) of empty AOT-based MEs and PPI-G2-loaded MEs were obtained by means of the computer-aided EPR analysis by adding 5-DSA (Chart 1B) to the mixtures. The probe's amphiphilic nature enables its localization between AOT molecules at the interface, reporting on the nearby environment of different structures. At pHs 13 and 8.6 5-DSA is fully ionized (carboxylate anion).[22] Thus, the carboxylate ions are fully hydrated in solution.[28] However, the EPR analysis indicates that the doxyl group is located in the well-packed lipid structure with its tail solubilized by the surfactant tails and its carboxylate in the vicinity of the polar AOT headgroups (pK_a(stearic acid) = 7.45).[3]

The spectra of 5-DSA-loaded ME droplets in the absence and presence of PPI-G2 were compared with all the reference spectra obtained from 5-DSA in the various components constituting the mixture. Figure 1 shows, as examples, the experimental and computed spectra obtained for 5-DSA in water solution, in the absence and in the presence of 25 wt % PPI-G2. It must be noted that 5-DSA is poorly soluble in water and the low-intensity spectrum that is obtained in water is characterized by a lower microviscosity and a higher polarity with respect to that in the presence of PPI-G2 (parameters reported in Table 1). Indeed, the polarity parameter of 5-DSA in distilled water is the highest ($\langle A \rangle$ = 15.78 G) compared to all the other reference samples, while its microviscosity parameter is the lowest (τ_{perp} = 0.1 ns).

The 5-DSA solubility in dendrimer solutions increases with respect to pure water because the 5-DSA chain may be partially hosted into the low polar dendrimer internal structure. Figure 2 shows the proposed interaction between the 5-DSA probe and the PPI-G2 dendrimer.

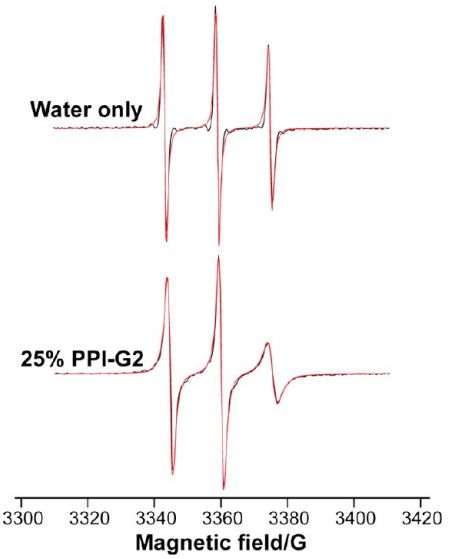

Figure 1. Experimental (black lines) and computed (red lines) spectra obtained for 5-DSA in water solution (0.1 mM), in the absence and in the presence of 25 wt % PPI-G2.

Table 1. Polarity (Hyperfine Coupling Constant $\langle A \rangle$) and Microviscosity (τ_{perp}) of the Reference Compositions[a]

sample	$\langle A \rangle$ (G)	τ_{perp} (ns)
water	15.78	0.10
water pH 8.6	15.78	0.10
5 wt % PPI-G2 in water pH 13	15.59	0.26
25 wt % PPI-G2 in water pH 13	15.40	0.835
5 wt % PPI-G2 in water pH 8.6	15.75	0.14
AOT−heptane mixture (1:1.5)	14.17	1.87
AOT−decane mixture (1:1.5)	14.26	3.25

[a]Accuracy ±2%. The order parameter in all samples is S = 0.

On the basis of the interaction between the probe and dendrimer, the microviscosity increases and the polarity slightly decreases with respect to water due to the interaction of the doxyl group with the amino groups of the dendrimer. Thus, as the dendrimer concentration increases from 5 to 25 wt %, the polarity decreases ($\langle A \rangle$ from 15.59 to 15.40 G). At pH 8.6 the polarity of the PPI-G2 solution is higher than at pH 13 because at pH 8.6 PPI-G2 is partially protonated at its terminal amino groups. Since the system is more charged, the nitroxide group is located in a more polar environment. For all the reference solutions (not MEs) such as water, PPI-G2 in water, and AOT/oil mixture, the order parameter was not needed in the spectral computation (S = 0). The microviscosity is higher once PPI-G2 is added to water (τ_{perp} = 0.26 ns versus 0.1 ns, respectively) and it rises as PPI-G2 content increases (τ_{perp} from 0.26 ns at 5 wt % to 0.835 ns at 25 wt %). This is in good agreement with the increase in the macroviscosity of PPI-G2 aqueous solutions. From these results, we learned that the probe weakly binds to the dendrimer. When the pH of the PPI-G2 solution is 8.6 (titrated with HCl), the microviscosity is somewhat lower (τ_{perp} = 0.14 ns).

AOT-in-heptane or decane forms reverse micelles. In these systems, 5-DSA environmental polarity ($\langle A \rangle$ = 14.17 and 14.26 G, respectively) is lower than polarity in pure water ($\langle A \rangle$ = 15.78 G), because the doxyl group inserts into reversed micellar interface (Table 1). The microviscosity is, as expected for the probes embedded into the micelles, relatively high (τ_{perp} = 1.87

dx.doi.org/10.1021/jp307616b | J. Phys. Chem. B 2012, 116, 12633−12640

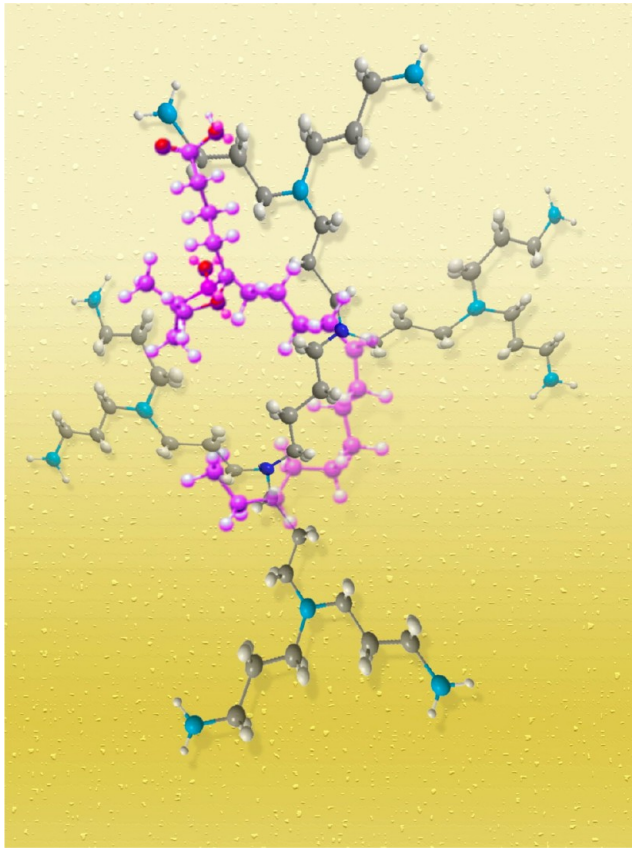

Figure 2. Tentative schematic illustration of the interaction of the 5-DSA probe with the PPI-G2 dendrimer. The probe molecule (in purple) is wrapped around the dendrimer (in blue) core, interacting with its inner functional groups.

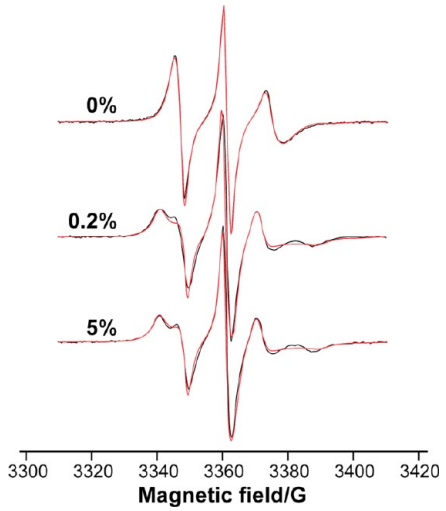

Figure 3. Experimental (black lines) and computed (red lines) EPR spectra of the 5-DSA probe (0.04 mM) in the ME formed by adding 24 wt % water to the AOT-in-oil reverse micelles in the absence and the presence of different quantities of PPI-G2 dendrimers. Top: no dendrimer. Middle: 0.2 wt % PPI-G2. Bottom: 5 wt % PPI-G2.

Table 2. Hyperfine Coupling Constant $\langle A \rangle$, Microviscosity (τ_{perp}), and Order Parameters (S) of the Systems[a]

PPI-G2 (wt %)	water (wt %)	type of oil	pH	$\langle A \rangle$ (G)	τ_{perp} (ns)	S
0	13	heptane	8.6	14.58	1.70	0
0	13	decane	8.6	14.50	1.32	0.14
0	13	heptane	13	14.58	1.70	0
0	24	heptane	13	14.50	1.32	0.14
0	24	decane	13	14.67	1.05	0.24
0.05	24	heptane	13	14.50	1.32	0.14
0.2	24	heptane	13	15.20	2.10	0.365
0.4	24	heptane	13	15.20	2.10	0.38
5	24	heptane	13	15.20	2.10	0.38
10	24	heptane	13	15.20	2.10	0.38
15	24	heptane	13	15.20	2.10	0.385
20	24	heptane	13	15.20	2.10	0.39
25	24	heptane	13	15.20	2.10	0.39

[a]Accuracy ±2%.

and 3.25 versus 0.1 ns, respectively; Table 1). It should be noted that the polarity of 5-DSA in AOT−heptane mixture ($\langle A \rangle$ = 14.17 G) is almost the same as in AOT−decane mixture ($\langle A \rangle$ = 14.26 G), while the microviscosity is much lower in AOT−heptane (τ_{perp} = 1.87 ns) than in AOT−decane (τ_{perp} = 3.25 ns). Heptane is smaller and shorter than decane, and thus the probe has more mobility due to weaker van der Waals interactions between the oil molecules.

When the W/O ME is formed by adding 24 wt % water to the AOT-in-oil reverse micelles, the spectral line shape changes significantly. Figure 3 shows, in the top spectrum, the experimental and computed spectra of the 5-DSA probe in the empty ME.

Polarity, microviscosity, and order parameter of empty (no PPI-G2) MEs (13 wt % and 24 wt % water phase; parameters listed in Table 2) are compared to those measured in pure water and AOT−oil mixtures (Table 1).

The polarities of 5-DSA in the empty MEs ($\langle A \rangle$ = 14.58 G for 13 wt % water and $\langle A \rangle$ = 14.50 G for 24 wt % water, Table 2) are lower than in pure water ($\langle A \rangle$ = 15.78 G, Table 1), but larger than in AOT−oil (heptane and decane) mixtures ($\langle A \rangle$ = 14.17 and 14.26 G, respectively; Table 1) as expected, due to the location of the probe in the AOT interface. Microviscosity is dependent on the droplet size. As the droplet size decreases the microviscosity increases. As a consequence, the microviscosities of the empty MEs (τ_{perp} = 1.70 ns for 13 wt % water, and τ_{perp} = 1.32 ns for 24 wt % water; see Table 2) are lower than AOT−oil (heptane and decane) mixtures (τ_{perp} = 1.87 and 3.25 ns, respectively; Table 1).

A further consequence of embedment of the spin probe in the AOT tail phase is that the order in the empty MEs is S = 0.14 (24 wt % water), which is higher than in AOT−oil mixtures (S = 0).

All the results of the empty MEs are well explained on the basis of the structure and organization of these systems, which is shown in Figure 4A.

In the following, we compare these results (empty ME) with those from the same systems loaded with PPI-G2.

3.1. Addition of PPI-G2 at Different Concentrations to the ME. In 24 wt % water, MEs (pH 13) loaded with only 0.05 wt % PPI-G2 (from the aqueous content), the polarity, microviscosity, and order parameter did not change in comparison to the empty ME (Table 2). However, once 0.2 wt % PPI-G2 was solubilized, the EPR signal changed, as shown in Figure 3, middle spectra, and in Table 2. From the figure and the table, it can be seen that all three parameters increased after addition of 0.2 wt % PPI-G2.

dx.doi.org/10.1021/jp307616b | J. Phys. Chem. B 2012, 116, 12633−12640

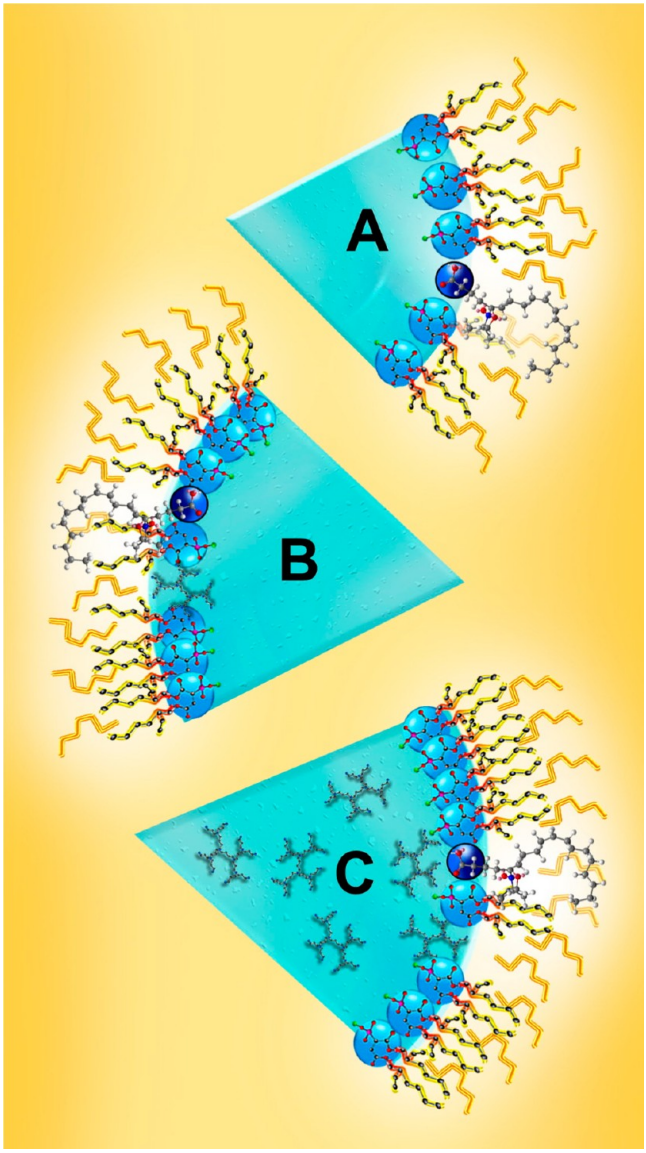

Figure 4. Proposed structural organization of the AOT-in-heptane, water, and 5-DSA ME (only a section of the droplet is shown) in the absence and the presence of the PPI-G2 dendrimer. The probe intercalates between the AOT molecules at the interface. (A) No dendrimer; (B) 0.2 wt % PPI-G2, one molecule of dendrimer per droplet penetrates the interface; (C) high dendrimer percentages, additional dendrimer molecules are dissolved in the aqueous core.

In our previous study,[33] it was found that PPI-G2 dendrimer molecules, although water soluble, are partially intercalated in the AOT/water interface. The dendrimer molecule that is intercalated in the interface behaves as a spacer between the AOT molecules. This provokes the 5-DSA chains that are squeezed between AOT molecules, which become more packed and ordered around the probe, and therefore microviscosity and order degree increased from τ_{perp} = 1.32 ns and S = 0.14 in the absence of the dendrimer, to τ_{perp} = 2.1 ns and S = 0.365, for 0.2 wt % PPI-G2 (Table 2). Contemporaneously, the dendrimer is interacting with the polar heads of both probe and surfactants, thus increasing the probe environmental polarity (from $\langle A \rangle$ = 14.50 G in the absence of the dendrimer to $\langle A \rangle$ = 15.20 G in the presence of 0.2 wt % dendrimer).

Figure 4B displays the structural variation in the ME droplets after addition of 0.2 wt % dendrimer as monitored by the 5-DSA probe.

The further question to be answered is why a PPI-G2 concentration higher than 0.05 wt % of dendrimer was needed to let the 5-DSA probe report about the structural variation provoked by the dendrimer. In order to understand this behavior, we calculated the mole ratios of AOT to PPI-G2 and to the probe and also the number of molecules of each of them per droplet of W/O for each concentration of the dendrimer[44,45] (Table 3). At 0.05 wt % and 0.2 wt % of PPI-G2 loading into 24 wt % aqueous phase ME, the molar ratio between AOT and PPI-G2 is very high (4400 and 1100, respectively) and the calculated number of PPI-G2 molecules per droplet is very small (0.06 and 0.23, respectively). This should mean that on average only one out of 16 or 4 droplets (respectively) contains one PPI-G2 molecule (Table 3). Yet, only above 0.05 wt % PPI-G2 is 5-DSA sensitive enough to detect the changes in the parameters caused by the dendrimer. In Figure 3, middle and bottom spectra, it can be seen that the first line is composed of two components. This points out that 5-DSA is embedded in two environments, one near the PPI-G2 dendrimer and the other far from the dendrimer. In the environment near the dendrimer, 5-DSA detects a more viscous and ordered environment. As PPI-G2 concentration increases, more 5-DSA is located close to PPI-G2.

The AOT to PPI-G2 ratio was progressively decreased by increasing the number of molecules of PPI-G2 from 0.23 to 45 per droplet (this corresponds to an increase of PPI-G2 concentration from 0.2 to 25 wt %, respectively). Yet, when PPI-G2 > 0.2 wt % was added, there was no change in polarity and microviscosity but an increase in the degree of order (parameters reported in Table 2). Figure 3, bottom spectrum, shows the experimental and computed spectra obtained for a loading of 5 wt % PPI-G2 in the ME constituted by 24 wt % water in heptane.

Table 3. Calculated Weight Percents, Moles, and Molar Ratios of AOT to PPI-G2

PPI-G2					no. of molecules per droplet		
wt % (from water)	wt % (from overall)	moles	AOT/PPI-G2 mole ratio	no. of droplets	AOT	PPI-G2	5-DSA
0	0	0	0	1.6×10^{18}	256	0	0.02
0.05	0.012	1.6×10^{-7}	4400	1.6×10^{18}	256	0.06	0.02
0.2	0.048	6.2×10^{-7}	1100	1.6×10^{18}	256	0.23	0.02
2	0.48	6.2×10^{-6}	110	1.6×10^{18}	261	2	0.02
5	1.2	1.6×10^{-5}	44	1.5×10^{18}	268	6	0.02
10	2.4	3.1×10^{-5}	22	1.4×10^{18}	284	13	0.02
20	4.8	6.2×10^{-5}	11	1.2×10^{18}	346	31	0.03
25	6	7.8×10^{-5}	9	1.0×10^{18}	393	45	0.03

dx.doi.org/10.1021/jp307616b | J. Phys. Chem. B 2012, 116, 12633−12640

The spectra changed little with an increase in the dendrimer content because the interface, in the presence of PPI-G2, has very limited possibility to pack and organize the AOT molecules in the droplet of a defined size.[17] Any addition of PPI-G2 molecules will force them to move to the aqueous core of the droplet, and thus no longer perturb the 5-DSA probe. In Figure 4B we schematically show our interpretation of the organization and integration of a single PPI-G2 molecule, per ME droplet, at the interface together with the probe. The curvature is not affected and the dendrimer molecule is accommodated at the interface. In Figure 4C we demonstrate the change in the location of the dendrimer with its increasing concentration in the ME.

These results are significant because they demonstrate that the ME interface has very limited capacity to encapsulate dendrimer molecules, and any excess of PPI-G2 molecules dissolves in the water phase. These findings are very good guidelines when designing a system with controlled release patterns of PPI-G2 as a function of its solubilization load. The PPI-G2 molecules residing at the ME interface should be released prior to the molecules soluble in the aqueous core of the ME.

To analyze the effect of type of oil, water content, and pH on the ME structure described in the next sections, it was possible to compute the spectra by taking the correlation time for the motion constant (τ_{perp} = 2.1 ns), only changing the molecular order and the polarity parameters. In this way, the S and $\langle A \rangle$ values are better compared among the various systems.

3.2. Effect of Type of Oil. Figure 5 shows, as examples, the experimental and computed spectra of 5-DSA (0.04 mM) in 5 wt % PPI-G2 loaded ME with 24 wt % water in dodecane as continuous phase, compared with the spectra obtained in heptane.

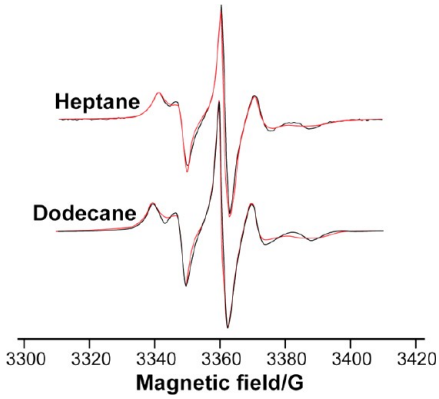

Figure 5. Experimental and computed spectra of 5-DSA (0.1 mM) in 5 wt % PPI-G2 loaded ME with 24 wt % water in dodecane as continuous phase, compared with the spectra obtained in heptane.

The polarity and order parameters at constant microviscosity used for the computations of the spectra in different oils and in the different experimental conditions are listed in Table 4. The order parameter increases as the chain length of the oil increases with both water contents and pH (S = 0.38 and 0.42 at pH 13, and S = 0.35 and 0.42 at pH 8.6, for heptane and dodecane, respectively, at 13 wt % water, for example). As expected, the order parameter reflects the improved packing of the droplets with the elongation of the chain length; that is, there is enhanced oil solvation of the surfactant tails, derived from strict packing of longer tails and stronger van der Waals interactions. In addition, because heptane has a shorter tail length, it penetrates between the AOT molecules and causes a decrease in the order.

Table 4. Hyperfine Coupling Constant $\langle A \rangle$ and Order Parameter (S) Obtained from the Computations of the EPR Spectra of 5-DSA (0.1 mM) in the ME Solutions of Three Types of Oil, Two pH Levels, and Three Water Contents, and 5 wt % PPI-G2[a]

type of oil	pH	water content (wt %)	$\langle A \rangle$ (G)	S
heptane	13	24	15.20	0.38
decane	13	24	15.20	0.41
dodecane	13	24	15.23	0.42
heptane	13	13	15.00	0.345
decane	13	13	15.20	0.39
dodecane	13	13	15.10	0.42
heptane	8.6	13	15.20	0.335
decane	8.6	13	15.20	0.38
dodecane	8.6	13	15.20	0.42
heptane	13	8	14.90	0.29
heptane	8.6	8	14.83	0.24

[a]The correlation time for the diffusion rotational motion, measuring the microviscosity, was taken to be constant in the computations (τ_{perp} = 2.1 ns). There are three water contents only at pH 13, because at pH 8.6, 13 wt % is the maximum water content that allows retaining the ME structure.

The proposed structural variations of the ME by changing the oil from heptane to dodecane are shown in Figure 6.

3.3. Effect of Water Content. The experimental and computed spectra of 5-DSA (0.04 mM) in 5 wt % PPI-G2

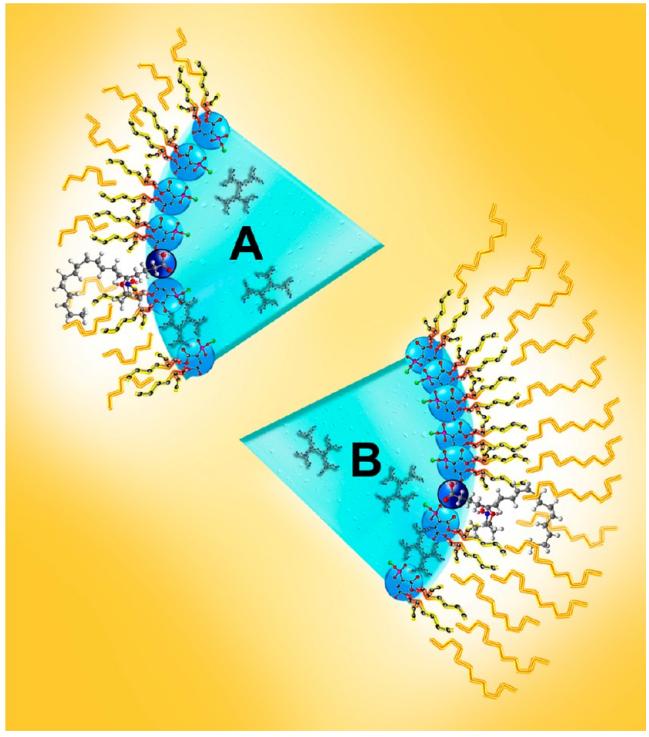

Figure 6. Proposed structural variations of the microemulsions by changing the oil from heptane (A) to dodecane (B). In heptane the oil molecules penetrate the AOT hydrophobic tails and prevent them from being ordered. Dodecane oil molecules have lesser penetration of the AOT tails and thus the interface is more ordered.

loaded into ME with 8, 13, and 24 wt % water in heptane are presented in Figure 7.

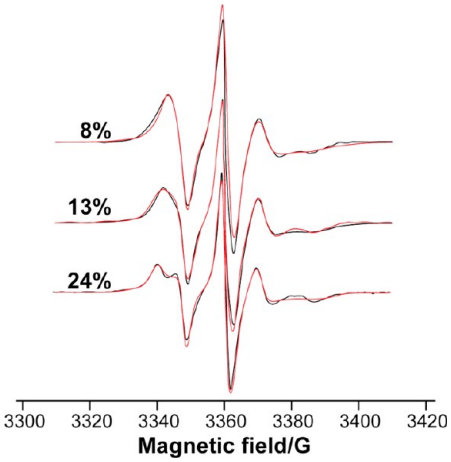

Figure 7. Experimental (black lines) and computed (red lines) spectra of 5-DSA (0.04 mM) in 5 wt % PPI-G2 loaded into ME with 8, 13, and 24 wt % water in heptane.

The polarity and degree of order of the systems at constant microviscosity and at three ME swelling levels obtained by increasing the water content are summarized in Table 4. It is clear that the increase in the water quantity provokes the increase of both the polarity ($\langle A \rangle$ from 14.90 to 15.20 G at pH 13, and $\langle A \rangle$ from 14.83 to 15.00 G at pH 8.6, for water contents from 8 to 24 wt %, respectively) and the degree of order (S from 0.29 to 0.38 at pH 13, and S from 0.24 to 0.335 at pH 8.6, for water content from 8 to 24 wt %, respectively). This is in line with the higher curvature of the swelled droplets at high water content, which provokes a higher packing (and consequent ordering) of the surfactants, as shown in Figure 8.

3.4. Effect of pH. The pH effect is not very significant. In some of the samples, the polarity at pH 8.6 is higher than at pH 13, and the order is somewhat lower at pH 8.6 (Table 4). A small amount of the positively charged external amino groups of the PPI-G2 molecules at pH 8.6 electrostatically interacts with the sulfonate headgroups of the AOT molecules at the interface. These interactions decrease the hydration (salting out) of the AOT headgroups by water. This effect can explain the decrease in the order at pH 8.6.

4. CONCLUSIONS

Computer-aided EPR analysis of the spectra of the 5-DSA probe embedded into the AOT surfactant layer provided significant information on the effects of changing ME composition on the microviscosity, polarity, and degree of order for systems unloaded and loaded with PPI-G2 dendrimers at increasing quantities.

The results indicate that above 0.2 wt % PPI-G2 the dendrimers saturated the AOT/water interface and affected its degree of order and microviscosity. At higher PPI-G2 content, the dendrimers dissolve in the aqueous core and have a very minor effect on the interface.

Parameters such as type of oil, water content, and pH influence the order and polarity of the microenvironment when different quantities of PPI-G2 are loaded into the MEs. As the oil's chain length becomes longer the order is higher. When water content is increased, both polarity and degree of order

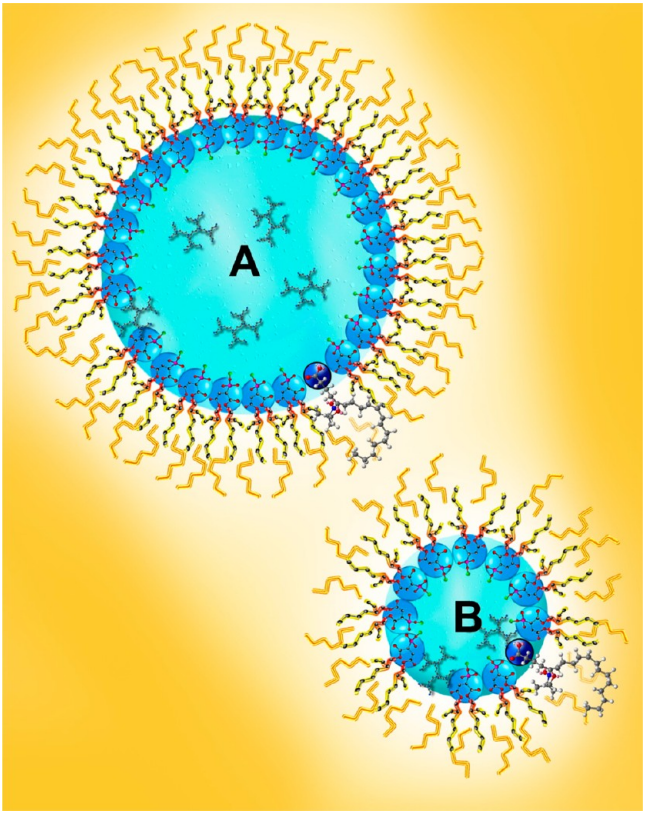

Figure 8. Proposed variation of nanostructure of the ME droplets by decreasing the water content: (A) 24 wt % water; (B) 8 wt % water. As water content increases, there are more defined borders, greater polarity, and increase in order degree.

increase. The influence of pH was not detected by 5-DSA probe, because it does not change the ME structure at the nitroxide site.

The improved understanding of the behavior of the dendrimer at the ME interface and in the core, when MEs are used as dendrimer nanocarriers and dendrimer-protecting capsules, is relevant for a better understanding of the release profile of a drug linked to dendrimers, or when the dendrimers are used for therapeutic purposes.

AUTHOR INFORMATION

Corresponding Author

*Tel.: +39-0722-304320 (M.F.O.); +972-2-658-6574/5 (N.G.). Fax: +39-0722-304222 (M.F.O.); +972-2-652-0262 (N.G.). E-mail: maria.ottaviani@uniurb.it (M.F.O.); garti@vms.huji.ac.il (N.G.).

Notes

The authors declare no competing financial interest.

⊥The results presented in this paper are part of S.R.'s fulfillment of the requirements for the M.Sc. degree in Applied Chemistry, The Hebrew University of Jerusalem.

REFERENCES

(1) Strey, R. *Colloid Polym. Sci.* **1994**, *272*, 1005−1019.
(2) Teo, B. M.; Ashokkumar, M.; Grieser, F. *J. Phys. Chem. B* **2008**, *112*, 5265−5267.
(3) Mao, S.; Chen, Z.; Fan, D.; An, X.; Shen, W. *J. Phys. Chem. A* **2012**, *116*, 158−165.
(4) Wolf, L.; Hoffmann, H.; Teshigawara, T.; Okamoto, T.; Talmon, Y. *J. Phys. Chem. B* **2012**, *116*, 2131−2137.

(5) Rozner, S.; Shalev, D. E.; Shames, A. I.; Ottaviani, M. F.; Aserin, A.; Garti, N. *Colloids Surf. B* **2010**, *77*, 22−30.
(6) Spernath, A.; Aserin, A. *Adv. Colloid Interface Sci.* **2006**, *128*, 47−64.
(7) Kogan, A.; Garti, N. *Adv. Colloid Interface Sci.* **2006**, *123*, 369−385.
(8) Walderhaug, H. *J. Phys. Chem. B* **2007**, *111*, 9821−9827.
(9) Wipf, R.; Kraska, M.; Spehr, T.; Nieberle, J.; Frey, H.; Stuehn, B. *Soft Matter* **2011**, *7*, 10879−10888.
(10) Bitan-Cherbakovsky, L.; Libster, D.; Ottaviani, M. F.; Aserin, A.; Garti, N. *J. Phys. Chem. B* **2012**, *116*, 2420−2429.
(11) Wolinsky, J. B.; Grinstaff, M. W. *Adv. Drug Delivery Rev.* **2008**, *60*, 1037−1055.
(12) Nanjwade, B. K.; Bechra, H. M.; Derkar, G. K.; Manvi, F. V.; Nanjwade, V. K. *Eur. J. Pharm. Sci.* **2009**, *38*, 185−196.
(13) Sebby, K. B.; Walter, E. D.; Usselman, R. J.; Cloninger, M. J.; Singel, D. J. *J. Phys. Chem. B* **2011**, *115*, 4613−4620.
(14) Shao, N.; Gong, X.; Chen, Q.; Cheng, Y. *J. Phys. Chem. B* **2012**, *116*, 5398−5405.
(15) Tomalia, D. A.; Naylor, A. M.; Goddard, W. A. *Angew. Chem., Int. Ed. Engl.* **1990**, *29*, 138−175.
(16) Maingi, V.; Kumar, M. V. S.; Maiti, P. K. *J. Phys. Chem. B* **2012**, *116*, 4370−4376.
(17) Dufes, C.; Uchegbu, I. F.; Schatzlein, A. G. *Adv. Drug Delivery Rev.* **2005**, *57*, 2177−2202.
(18) Choi, J. S.; Nam, K.; Park, J.; Kim, J. B.; Lee, J. K. *J. Controlled Release* **2004**, *99*, 445−456.
(19) Gajbhiye, V.; Palanirajan, V. K.; Tekade, R. K.; Jain, N. K. *J. Pharm. Pharmacol.* **2009**, *61*, 989−1003.
(20) Solassol, J.; Crozet, C.; Perrier, V.; Leclaire, J.; Beranger, F.; Caminade, A. M.; Meunier, B.; Dormont, D.; Majoral, J. P.; Lehmann, S. *J. Gen. Virol.* **2004**, *85*, 1791−1799.
(21) Klajnert, B.; Cortijo-Arellano, M.; Cladera, J.; Bryszewska, M. *Biochem. Biophys. Res. Commun.* **2006**, *345*, 21−28.
(22) Chauhan, A. S.; Diwan, P. V.; Jain, N. K.; Tomalia, D. A. *Biomacromolecules* **2009**, *10*, 1195−1202.
(23) Witvrouw, M.; Fikkert, V.; Pluymers, W.; Matthews, B.; Mardel, K.; Schols, D.; Raff, J.; Debyser, Z.; De Clercq, E.; Holan, G.; Pannecouque, C. *Mol. Pharmacol.* **2000**, *58*, 1100−1108.
(24) Gong, Y. H.; Matthews, B.; Cheung, D.; Tam, T.; Gadawski, I.; Leung, D.; Holan, G.; Raff, J.; Sacks, S. *Antiviral Res.* **2002**, *55*, 319−329.
(25) Chen, C. Z. S.; Beck-Tan, N. C.; Dhurjati, P.; van Dyk, T. K.; LaRossa, R. A.; Cooper, S. L. *Biomacromolecules* **2000**, *1*, 473−480.
(26) Pospisil, M.; Vannucci, L.; Fiserova, A.; Krausova, K.; Horvath, O.; Kren, V.; Mosca, F.; Lindhorst, T. K.; Sadalapure, K.; Bezouska, K. *Adv. Exp. Biol. Med.* **2001**, *495*, 343−347.
(27) Ottaviani, M. F.; Mazzeo, R.; Cangiotti, M.; Fiorani, L.; Majoral, J. P.; Caminade, A. M.; Pedziwiatr, E.; Bryszewska, M.; Klajnert, B. *Biomacromolecules* **2010**, *11*, 3014−3021.
(28) Klajnert, B.; Cangiotti, M.; Calici, S.; Majoral, J. P.; Caminade, A. M.; Cladera, J.; Bryszewska, M.; Ottaviani, M. F. *Macromol. Biosci.* **2007**, *7*, 1065−1074.
(29) Bitan-Cherbakovsky, L.; Libster, D.; Aserin, A.; Garti, N. *J. Phys. Chem. B* **2011**, *115*, 11984−11992.
(30) Cheng, Y. Y.; Xu, T. W. *Eur. J. Med. Chem.* **2008**, *43*, 2291−2297.
(31) Chen, C. Z. S.; Cooper, S. L. *Biomaterials* **2002**, *23*, 3359−3368.
(32) Scherrenberg, R.; Coussens, B.; van Vliet, P.; Edouard, G.; Brackman, J.; de Brabander, E.; Mortensen, K. *Macromolecules* **1998**, *31*, 456−461.
(33) Nir, I.; Aserin, A.; Libster, D.; Garti, N. *J. Phys. Chem. B* **2010**, *114*, 16723−16730.
(34) Kogan, A.; Rozner, S.; Mehta, S.; Somasundaran, P.; Aserin, A.; Garti, N.; Ottaviani, M. F. *J. Phys. Chem. B* **2009**, *113*, 691−699.
(35) Rozner, S.; Kogan, A.; Mehta, S.; Somasundaran, P.; Aserin, A.; Garti, N.; Ottaviani, M. F. *J. Phys. Chem. B* **2009**, *113*, 700−707.
(36) Baglioni, P.; Rivaraminten, E.; Dei, L.; Ferroni, E. *J. Phys. Chem.* **1990**, *94*, 8218−8222.
(37) Zuev, Y. F.; Vylegzhanina, N. N.; Zakhartchenko, N. L. *Appl. Magn. Reson.* **2003**, *25*, 29−42.
(38) Ottaviani, M. F.; Daddi, R.; Brustolon, M.; Turro, N. J.; Tomalia, D. A. *Appl. Magn. Reson.* **1997**, *13*, 347−363.
(39) Mishraki, T.; Ottaviani, M. F.; Shames, A. I.; Aserin, A.; Garti, N. *J. Phys. Chem. B* **2011**, *115*, 8054−8062.
(40) Wines, T. H.; Somasundaran, P.; Turro, N. J.; Jockusch, S.; Ottaviani, M. F. *J. Colloid Interface Sci.* **2005**, *285*, 318−325.
(41) Budil, D. E.; Lee, S.; Saxena, S.; Freed, J. H. *J. Magn. Reson., Ser. A* **1996**, *120*, 155−189.
(42) Schneider, D. J.; Freed, J. H. Calculating Slow Motional Magnetic Resonance Spectra: A User's Guide; In *Spin Labeling Theory and Applications*, Vol. *8*; Berliner, L. J., Reuben, J., Eds.; Plenum Press: New York, 1989; pp 1−76.
(43) Kabanov, V. A.; Zezin, A. B.; Rogacheva, V. B.; Gulyaeva, Z. G.; Zansochova, M. F.; Joosten, J. G. H.; Brackman, J. *Macromolecules* **1998**, *31*, 5142−5144.
(44) Nir, I. "Investigation of Microemulsions by the TDS Method (Time Domain Dielectric Spectroscopy)", The Hebrew University of Jerusalem, 1997.
(45) Vandijk, M. A.; Joosten, J. G. H.; Levine, Y. K.; Bedeaux, D. *J. Phys. Chem.* **1989**, *93*, 2506−2512.